Structural, Photophysical, and Conductive Properties of *n*-Hexyl Substituted Hybrid Polysilylene−Polysilyne Networks

Cornelis A. van Walree, Thomas J. Cleij, Leonardus W. Jenneskens,* and Edward J. Vlietstra

Debye Institute, Department of Physical Organic Chemistry, Utrecht University, Padualaan 8, 3584 CH Utrecht, The Netherlands

Garrelt P. van der Laan and Matthijs P. de Haas

Radiation Chemistry Department, IRI, Delft University of Technology, Mekelweg 15, 2629 JB Delft, The Netherlands

Egbertus T. G. Lutz

Department of Analytical Molecular Spectroscopy, Utrecht University, Sorbonnelaan 16, 3584 CA Utrecht, The Netherlands

Received March 19, 1996; Revised Manuscript Received August 20, 1996[⊗]

ABSTRACT: Structural, photophysical, and charge transport properties of *n*-hexyl substituted polysilylenes containing 5, 33 or 67% *n*-hexylsilyne branching points were investigated. According to WAXD, DSC, and vibrational studies, introduction of branching points partially reduces the high degree of crystallinity of linear poly(di-*n*-hexylsilylene). A thermal transition occurs in all polymers, which leads to solid state thermochromic behavior. Solution thermochromism is also observed. It is shown that in the partially branched polymers the narrow band gap of polysilynes is accompanied by an exciton delocalization approaching that of linear polysilylenes. In the solid state, charge carrier mobilities, determined with the pulse-radiolysis time-resolved microwave conductivity technique, are high but decrease with increasing branching. They range from 1.5×10^{-5} for the linear polymer to 7.6×10^{-7} m^2 V^{-1} s^{-1} for the polymer with 67% branching sites. At the thermal transition an abrupt drop in the mobility is observed, of which the magnitude decreases with increasing branching. The branching points appear to act as scattering points for both exciton and charge carrier migration.

Introduction

Silicon-based materials attract considerable interest due to their interesting optical and electronic properties, which are strongly related to the dimensionality of the silicon backbone structure.[1,2] For instance, 3-dimensional crystalline silicon is an indirect band gap (1.1 eV) semiconductor, and luminescence is thus forbidden. Charge carrier mobilities are high, in the range of 0.1 m^2 V^{-1} s^{-1}. In noncrystalline forms of 3-dimensional silicon, such as (hydrogenated) amorphous and porous silicon, a *quasi*-indirect band gap of *ca.* 1.7 eV is found and both photo- and electroluminescence have been observed.[2−6] In amorphous silicon, charge carrier mobilities are in the range of 10^{-4}−10^{-3} m^2 V^{-1} s^{-1}.[7]

The optical properties of amorphous silicon are mimicked in branched and ladder silicon backbone polymers[8] and polysilynes $(SiR)_m$.[9−16] The latter polymers are proposed to consist of *pseudo*-2-dimensional, sheetlike silicon networks, in which each silicon atom is bonded to three other silicon atoms and one organic side group R. Recently, hyperbranched, dendritic structures have also been suggested.[17] Band gaps of polysilynes are on the order of 3 eV, and a weak, broad photoluminescence similar to that of amorphous semiconductors is found.

The intriguing photophysical properties of 1-dimensional polysilylenes $(SiRR')_m$ have been studied extensively in the last decade.[18,19] These polymers exhibit a strong absorption and photoluminescence in the near UV region, unusual for a σ-bonded framework. In addition, other interesting (photo)physical properties, such as thermochromism, photo-[20] and dark conductivity upon doping,[21] and third-order optical nonlinearities,[22,23] have been reported.[18] These features are based on the occurrence of σ-delocalization, rationalized in terms of resonance interactions between sp^3 hybrids, along the silicon chain. Conformational changes as a function of temperature are responsible for the thermochromism by affecting conjugation. Mobilities of charge carriers in polysilylenes, which are presumably holes, are high.[24−31] Mobility values determined with the pulse-radiolysis time-resolved microwave conductivity (PR-TRMC) technique range from 10^{-5} to 10^{-7} m^2 V^{-1} s^{-1} and are markedly dependent on the silicon backbone conformation.[27,29,30] Moreover, charge migration was shown to be favored in the direction of the silicon backbone.[28]

Here we report about the structural, optical, and conductive properties of *n*-hexyl substituted polysilylenes with various degrees of branching points incorporated, *i.e.*, polymers with the general formula $[Si(C_6H_{13})_n]_m$ with $n = 2$ (**1**), 1.95 (**2**), 1.67 (**3**), 1.33 (**4**), and 1 (**5**). These hybrid polysilylene−polysilyne networks cover the regime between 1-dimensional ($n = 2$) and *pseudo*-2-dimensional ($n = 1$) silicon backbones and can be regarded as polymeric analogues of recently reported dendritic oligosilylenes.[32−34] Structural and thermal properties have been studied using wide angle X-ray diffraction (WAXD), differential scanning calorimetry (DSC), and infrared (IR) and Raman spectroscopy. Optical properties, both in solution and in the solid state, have been investigated with UV and fluorescence spectroscopy. Charge migration in polymers **1**−**4** has been evaluated with use of the PR-TRMC technique. As the branched polysilylenes will be seen to undergo a thermal transition, attention is paid to the optical and

* Address correspondence to this author.

[⊗] Abstract published in *Advance ACS Abstracts,* October 1, 1996.

S0024-9297(96)00407-X CCC: $12.00

conductive characteristics in both their low temperature (LT) and high temperature (HT) structural phases.

Experimental Section

General. NMR spectra were recorded with a Bruker AC 300 spectrometer at 300 MHz for ^{1}H NMR, 75 MHz for ^{13}C, and 60 MHz for ^{29}Si NMR. ^{29}Si NMR spectra were recorded using a proton decoupled inverse gated pulse sequence with a relaxation delay of 15 s and referenced to internal TMS. Use was made of chromium(III) acetylacetonate as relaxation reagent. Gel permeation chromatography (GPC) was performed on a Shodex KF-804 column equipped with a Thermo Separation Products Spectra Series 200 pump. Molecular weights are given relative to polystyrene standards. Elemental analyses were carried out at Kolbe Microanalytisches Laboratorium, Mülheim an der Ruhr, Germany. DSC measurements were performed on a Mettler DSC 12E apparatus at scan rates of 5 °C·min^{-1}. WAXD patterns were collected on a Enraf-Nonius FR 590 diffractometer. Powdered samples were irradiated for 20 min with Fe Kα radiation (1.9373 Å). The 2θ region between 7.5° and 55° was scanned in 0.03° steps. The used neutron activation analysis technique is described elsewhere.[35,36]

Infrared (IR) Spectroscopy. IR spectra were recorded on a Perkin Elmer 2000 FT-IR spectrometer in transmission mode. Films cast on KBr discs were heated using a programmable variable temperature accessory (accuracy 0.1 °C) constructed in cooperation with Anatech bv, Sittard, The Netherlands. Spectra were recorded with 2 cm^{-1} optical spectral resolution and medium apodization and were averaged from 16 scans. Before measurement, films were annealed at −10 °C in order to ensure that polymers were in their low temperature phase.

FT-Raman Spectroscopy. Spectra were collected on a Perkin Elmer System 2000 NIR FT-Raman spectrometer equipped with a diode pumped Nd:YAG laser (1064 nm, CW pulse duration) and an InGaAs detector. Depending on the emissivity, use was made of laser powers of 50 or 100 mW and optical spectral resolutions of 2 or 4 cm^{-1}, respectively; spectra were averaged from 24 scans. Samples were measured as either powder or gel in a home-built circular 2 mm aluminium probe developed for 180° signal collection and were heated using a hot air blower. Temperatures were measured with a Comark 9001 digital thermometer containing a type K thermocouple. To establish that during measurement polymers were in their high temperature phase, the temperature was checked before and after the measurements.

UV Spectroscopy. Room temperature solution UV spectra were recorded on a Varian Cary 1 apparatus in spectrophotometric grade THF. Variable temperature solution UV spectra were obtained with a Varian Cary 5 UV−vis−NIR spectrophotometer in spectrophotometric grade hexane. Use was made of a home-built closed sample compartment equipped with a gas in- and outlet, a brass cuvette holder, and quartz windows. The solution temperature was regulated by flushing with cooled nitrogen gas and conducting a current through the brass block. The temperature of the sample was monitored with an Ebro TTX 1082 NiCr thermocouple pending in the solution *via* drilled stoppers. Film UV spectra were also collected on a Varian Cary 5 spectrophotometer. Thermochromic measurements were performed on films cast on polished quartz plates, kept in a modified Linkam THMS hot stage controlled by a Linkam TMS 91 temperature regulator.

Fluorescence Spectroscopy. Steady state fluorescence spectra were obtained on a Spex Fluorolog apparatus. Fluorescence quantum yields[37] were determined relative to 9,10-diphenylanthracene in cyclohexane ($\Phi_{fl} = 0.90$) upon 337 nm excitation. Solutions in spectrophotometric grade THF were degassed by purging with argon during 15 min. Solid state fluorescence spectra were recorded in front-face geometry on films cast on polished quartz plates. Films were heated by means of a hot air blower. Fluorescence lifetimes were determined using a Laser Photonics LN 1000 nitrogen laser (337.4 nm, 0.8 ns FWHM), a Jobin Yvon monochromator, and an ITL TF1850 photodiode. In order to reduce photodecomposition of the polymers, only one excitation pulse was given at each monitored emission wavelength.

Pulse-Radiolysis Time-Resolved Microwave Conductivity.[38−40] For PR-TRMC measurements, polymers were contained in a piece of rectangular waveguide (the cell) closed at one end with a copper plate. The volume fraction occupied by the polymers was calculated from the sample weight, its estimated density (1 g·cm^{-3}), and the known volume of the cell. Samples were ionized by pulsed irradiation with 3-MeV electrons generated by a Van de Graaff accelerator. The pulse width was varied from 0.5 to 10 ns; the deposited energy per pulse was in the range of 1−20 Gy (1−20 J·kg^{-1}) as determined with Far West Technology-92 radiochromic film dosimeters.[41] Total accumulated radiation doses on samples typically were 20 kGy; significant (10%) radiation damage on polysilylenes has been found to occur above 45 kGy.[42] The cell was flushed with SF_6 gas in order to scavenge free electrons formed by ionization of air.

Radiation induced conductivity changes ($\Delta\sigma$) were monitored by time-resolved measurement of changes in reflected microwave power using microwave frequencies of 26.5−38 GHz. Changes in the output of the microwave detector were measured with either a Tektronix 7912 oscilloscope for conductivity changes on a nanosecond time scale or a tandem combination of a Tektronix 2205 oscilloscope (7A13 plug-in) and a Sony/Tektronix RTD 710 digitizer for periods up to milliseconds. The absolute value of the conductivity was obtained from its frequency dependence using a fitting procedure described previously.[38,39]

Syntheses. Representative Example [Si(C$_6$H$_{13}$)$_{1.33}$]$_m$ (4). In an argon atmosphere, sodium (1.16 g, 50.5 mmol) was dispersed in boiling toluene (60 mL, freshly distilled from sodium−benzophenone) by vigorous stirring, in the presence of 12-crown-4 (0.20 g, 1.15 mmol). Oven dried glassware was used. Subsequently, a mixture of dichlorodi-*n*-hexylsilane (1.80 g, 6.7 mmol) and trichloro-*n*-hexylsilane (2.92 g, 13.3 mmol) was added dropwise during 20 min (**Caution:** *a strongly exothermic reaction occurs*). The reaction mixture was refluxed for 100 min, during which a purple color developed. After cooling to room temperature, methanol (20 mL) was added. The mixture was poured into methanol (200 mL), upon which a viscous wax-like liquid separated. This precipitate was successively triturated with methanol, washed with water, dissolved in THF, and reprecipitated from THF−methanol, 1:2 v/v. Yield 0.82 g (29%) of a yellow gel-like substance. ^{1}H NMR (300 MHz, toluene-d_8) δ 1.74 (br), 1.47 (br), 0.99 (br); ^{13}C NMR (75 MHz, toluene-d_8) δ 35.2, 33.9, 32.5, 32.2, 30.5, 28.4, 23.5, 23.2, 15.9, 14.4; ^{29}Si NMR (60 MHz, toluene-d_8) δ −23.9, −61 (broad); IR (film on KBr disc, cm^{-1}) 2957, 2924, 2872, 2857, 1467, 1378, 1100, 1043, 760, 727, 668. Anal. Calcd for (C$_6$H$_{13}$)$_{1.33}$Si: C, 67.84; H, 12.33; Si, 19.83. Found: C, 67.66; H, 12.25; Si, 19.95. GPC (THF *vs* polystyrene): M_w 2.5 × 10^4, polydispersity 2.7.

[Si(C$_6$H$_{13}$)$_2$]$_m$ (1). Yield 55% of a white solid. ^{1}H NMR (300 MHz, benzene-d_6) δ 1.90 (br), 1.73 (br), 1.54 (br), 1.06 (br); ^{13}C NMR (75 MHz, benzene-d_6) δ 35.3, 32.6, 28.5, 23.5, 16.0, 14.5; ^{29}Si NMR (60 MHz, benzene-d_6) δ −24.1; IR (film on KBr disc, cm^{-1}) 2954, 2921, 2871, 2856, 1469, 1377, 1176, 1104, 756, 750, 727, 718, 667. Anal. Calcd for (C$_6$H$_{13}$)$_2$Si: C, 72.64; H, 13.21; Si, 14.15. Found: C, 72.81; H, 13.15; Si, 14.26. GPC (THF *vs* polystyrene) showed an essentially bimodal distribution: M_w 4.4 × 10^5, polydispersity 1.2 (27% by area), and M_w 6.5 × 10^4, polydispersity 1.7 (73%).

[Si(C$_6$H$_{13}$)$_{1.95}$]$_m$ (2). Yield 52% of a white solid. ^{1}H NMR (300 MHz, benzene-d_6) δ 1.89 (br), 1.73 (br), 1.53 (br), 1.06 (br); ^{13}C NMR (75 MHz, benzene-d_6) δ 35.2, 32.6, 28.5, 23.5, 16.0, 14.5; ^{29}Si NMR (60 MHz, benzene-d_6) δ −24.0; a broad signal near −60 ppm could not be detected; IR (film on KBr disc, cm^{-1}) 2970, 2940, 2870, 1470, 1385, 1170, 1100, 950, 758, 726, 660. Anal. Calcd for (C$_6$H$_{13}$)$_{1.95}$Si: C, 72.38; H, 13.16; Si, 14.46. Found: C, 72.31; H, 13.04; Si, 14.38. GPC (THF *vs* polystyrene): M_w 9.3 × 10^5, polydispersity 1.2 (22%), and M_w 6.8 × 10^4, polydispersity 2.4 (78%).

[Si(C$_6$H$_{13}$)$_{1.67}$]$_m$ (3). Yield 23% of a yellow gel. ^{1}H NMR (300 MHz, benzene-d_6) δ 1.80 (br), 1.48 (br), 1.01 (br); ^{13}C NMR (75 MHz, benzene-d_6) δ 35.2, 33.8, 32.5, 32.1, 28.4, 23.4, 23.1,

Scheme 1

$$x\ Cl_2Si(C_6H_{13})_2 + y\ Cl_3Si(C_6H_{13}) \xrightarrow[12\text{-crown-4}]{Na\ /\ toluene} [Si(C_6H_{13})_n]_m \quad n = 1 + x/(x+y)$$

15.9, 14.4; ^{29}Si NMR (60 MHz, benzene-d_6) δ −24.5, −64 (broad); IR (film on KBr disc, cm^{-1}) 2956, 2923, 2872, 2857, 1469, 1378, 1175, 1095, 1000, 756, 727, 669. Anal. Calcd for $(C_6H_{13})_{1.67}Si$: C, 70.64; H, 12.84; Si, 16.52. Found: C, 70.75; H, 12.72; Si, 16.66. GPC (THF *vs* polystyrene): M_w 3.4 × 10^4, polydispersity 3.7.

$[Si(C_6H_{13})]_m$ (5). Yield 66% of a yellow solid. ^{1}H NMR (300 MHz, toluene-d_8) δ 1.56 (br), 1.04 (br); ^{13}C NMR (75 MHz, toluene-d_8) δ 34.9, 32.4, 23.4, 14.4; ^{29}Si NMR (60 MHz, benzene-d_6) δ −72 (broad); IR (KBr, cm^{-1}) 2957, 2924, 2872, 2857, 1467, 1378, 1170, 1097, 953, 760, 724, 672. Anal. Calcd for $(C_6H_{13})Si$: C, 63.63; H, 11.57; Si, 24.80. Found: C, 43.80; H, 8.85; Si, 21.22; O, 23.48. GPC (THF *vs* polystyrene): M_w 1.2 × 10^4, polydispersity 2.5.

Results and Discussion

Synthesis. Polymers **1**−**5** were synthesized by Wurtz-type condensation of mixtures of dichlorodi-*n*-hexylsilane and trichloro-*n*-hexylsilane with a sodium dispersion (0.95 equiv) in boiling toluene, 12-crown-4 being present as catalyst (Scheme 1).[11]

Polymers were obtained as white (**1**, **2**) to yellow (**3**, **4**, **5**) powders or gels that are soluble in common organic solvents such as hexane, tetrahydrofuran (THF), and benzene. Polymer **1** shows the usual trimodal GPC weight distribution,[18,43] with peak molecular weights of 4.4 × 10^5 and 6.5 × 10^4; the third signal, assigned to cyclic oligomeric fractions, appeared as a small shoulder. With increased branching, the weight distribution becomes more monomodal, and peak molecular weights decrease (*e.g.*, M_w = 2.5 × 10^4 for **4**). It should be noted that actual molecular weights of the branched polymers may be higher, since the GPC molecular weights are derived from linear polystyrene standards.[10,15] ^{29}Si NMR spectra of the hybrid networks display a sharp peak around −24 ppm originating from the silylene moieties $Si(C_6H_{13})_2$, and a very broad, weak signal near −60 ppm attributed to the silyne units $Si(C_6H_{13})$.[10]

Elemental analyses of the polymers are in excellent agreement with the monomer feed ratios. In the case of **5** (n = 1), however, reproducibly an oxygen content of *ca.* 23.5% was found.[44] The excellent elemental analyses of polymers **2**−**4** indicate that the dichloro- and trichlorosilane monomers are equally reactive under the reaction conditions used. The polymers are therefore likely to contain di-*n*-hexylsilylene and *n*-hexylsilyne units in a random order. As described below, this is further supported by the structural, photophysical, and conductive properties of the hybrid networks. Another contemplation supporting this view is that when mixtures or blocks of linear and totally branched structures had been formed, separation by precipitation should have occurred since the linear parts are far better soluble.

The excellent agreement between the polymer compositions and the monomer feed ratios differs from data on poly(methylphenylsilylenes) containing phenylsilyne branching points, where deviations from the feed ratio were found.[12] Presumably this is a consequence of the different reduction potentials of the dichloromethylphenylsilane and trichlorophenylsilane monomers, which results in unequal reactivities during polymerization.[43,45] Apparently, reduction potentials of dichlorodi-*n*-hexylsilane and trichloro-*n*-hexylsilane are not very different.

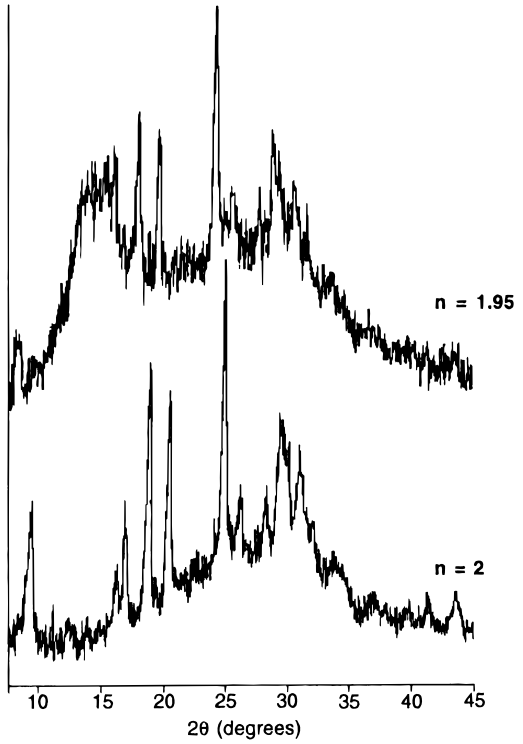

Figure 1. X-ray diffraction patterns of polymers **1** (n = 2, bottom) and **2** (n = 1.95, top).

Table 1. Main *d* Spacings (Å) in Polymers 1 (n = 2) and 2 (n = 1.95)

1			2		
2θ (deg)	d (Å)	intensity[a]	2θ (deg)	d (Å)	intensity[a]
9.43	11.8	0.28	9.00	12.3	0.26
			14.9	7.5	smeared
16.27	6.84	0.17	15.67	7.10	0.47
16.89	6.59	0.28	16.57	6.72	0.45
18.76	5.94	0.73	18.45	6.04	0.55
20.37	5.48	0.54	20.06	5.56	0.50
24.74	4.52	1	24.49	4.57	1
26.12	4.28	0.19	25.88	4.32	0.15
28.15	3.98	0.21	27.98	4.00	0.15
29.26	3.83	0.31	28.97	3.87	0.32
29.89	3.75	0.29	29.58	3.79	0.36
30.81	3.64	0.26	30.73	3.65	0.36

[a] Relative intensity by area.

Structural and Thermal Properties. As poly(di-*n*-hexylsilylene) (**1**) is a semicrystalline polymer,[46] it is worthwhile to consider the effect of the presence of branching points on its crystallinity. Powder X-ray diffraction (WAXD) patterns of polymers **1** and **2** are shown in Figure 1.[47] The *d* spacings found for **1** (Table 1) are in good agreement with previously reported data;[46] the only discrepancy is that the most intensive reflection, reported to occur at d = 8.9 Å, is absent in our sample. The 4.52 Å spacing is characteristic of the packing of *trans* planar (*antiperiplanar*) alkyl chains, while the 3.98 Å spacing, the chain repeat distance, is consistent with an *all-trans* silicon backbone conformation.[48] Polymer **2** (n = 1.95) is semicrystalline as well, but the sharp reflections are superimposed on broad halos. Hence, considerable amorphous character is already induced by incorporation of 5% branching points. Reflections are somewhat shifted to smaller angles with respect to those of **1**, particularly in the small angle region (2θ < 20°). This suggests that both the side chain crystallinity and the *all-trans* backbone conformation are not significantly affected

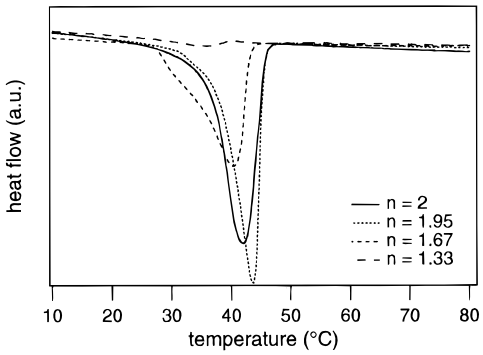

Figure 2. DSC thermograms of polymers **1** (n = 2), **2** (n = 1.95), **3** (n = 1.67), and **4** (n = 1.33) upon heating.

Table 2. DSC Transitions of Polymers $[Si(C_6H_{13})_n]_m$

polymer (n)	T_h[a] (°C)	ΔH[b] (kJ·mol^{-1})	T_c[c] (°C)
1 (2)	41	−14.7	26
2 (1.95)	42	−12.2	26
3 (1.67)	39	−8.7	24
4 (1.33)	35	−0.5	17

[a] Transition temperature (minimum of the DSC curve) upon heating. [b] Transition enthalpy per repeating unit upon heating. [c] Transition temperature (maximum of the DSC curve) upon cooling.

by the branching sites, but that the interchain packing is perturbed.

Differential scanning calorimetry (DSC) revealed that polymers **1**−**4** all exhibit a first-order phase transition (Figure 2 and Table 2). The transition shifts to lower temperatures with increased branching, while the transition enthalpy decreases. The enthalpy reduction is however much stronger than anticipated from the relative number of side chains. For polymer **4** the transition enthalpy is only −0.5 kJ·mol^{-1}, a factor of 29 less than that of **1**. All polymers exhibit hysteresis, *i.e.*, the transition temperature is significantly lowered upon cooling. The extent of hysteresis increases slightly when going from **1** to **4**.

The thermal transition of polymer **1** has been assigned to order−disorder phenomena ("melting") of the *n*-hexyl side chains,[18,46] which is followed by a conformational change of the backbone; a hexagonal liquid crystalline phase (mesophase) with a *gauche*-like backbone is adopted (see also IR and Raman spectroscopy).[49] In the branched polymers melting of the side chains appears to occur as well, but as indicated by the strongly reduced transition enthalpy, only a fraction of the side chains participates. Hence, in line with the WAXD results, incorporation of branching points results in a loss of crystallinity.

As vibrational transitions are highly sensitive to conformational structure, the loss of crystallinity upon incorporation of branching points was further investigated using temperature dependent IR and Raman spectroscopy. Owing to their complementary nature, IR spectroscopy predominantly monitors side chain effects, whereas Raman spectroscopy is a suitable tool to study main chain phenomena.[46,50] Characteristic IR spectral features associated with thermal transitions are observed in the 800−600 cm^{-1} spectral region comprising the CH_2 rock modes around 755 and 725 cm^{-1} and the Si−C stretch mode around 668 cm^{-1} (Figure 3). In the IR spectra of the linear polymer **1** in its low temperature (LT) phase the CH_2 rock bands, being sensitive to the packing of the methylene groups, split into two components as a result of interchain coupling. A comparable

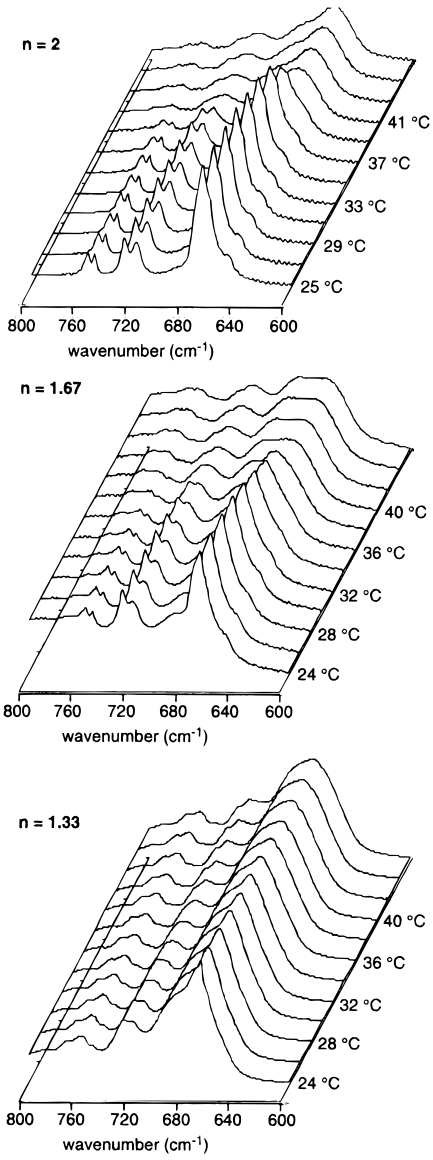

Figure 3. Temperature dependent IR spectra of polymers **1** (n = 2, top), **3** (n = 1.67, middle), and **4** (n = 1.33, bottom) in the region 800−600 cm^{-1}.

splitting has been observed for crystalline polyethylene.[51,52] In addition, Figure 3 reveals that in the LT phases bands broaden and the interchain coupling disappears concomitant with an increasing degree of branching, reflecting a gradual loss of side chain packing. In the case of **4**, LT spectra show a superposition of small narrow peaks and broad bands. Although its structure is mainly amorphous, ordered side chains must still be present in this polymer. Upon heating polymers **1**−**4**, bands broaden drastically in the temperature range where the DSC transitions occur, although the effect is less pronounced for **3** and **4**. It is thus shown that in common with the linear polymer **1** the thermal transitions of **3** and **4** are associated with melting of the ordered fraction of the side chains.

Apart from side chain signals between 1500 and 700 cm^{-1}, the most representative Raman bands are those corresponding to the symmetric Si−C stretch at 690 cm^{-1} and the Si−Si stretch vibrations around 493 (symmetric) and 373 cm^{-1} (asymmetric),[50,53] respectively (Figure 4). In the spectrum of **1** these bands are intense and narrow. The unusual large intensity of the 690 cm^{-1} band has been accounted for by mixing of Si−C

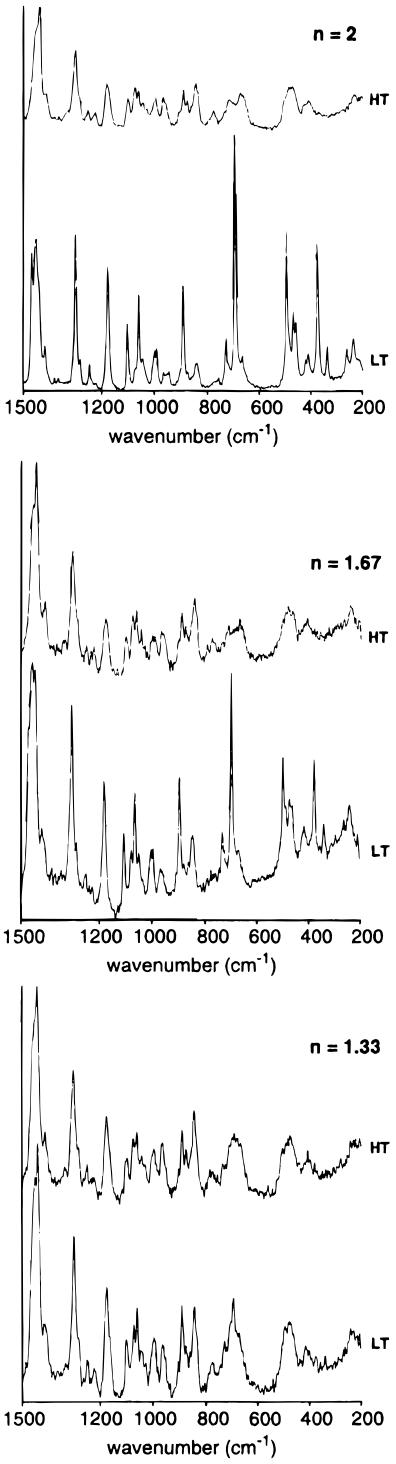

Figure 4. FT-Raman spectra in the region 1500−200 cm^{-1} of polymers **1** (n = 2, top), **3** (n = 1.67, middle), and **4** (n = 1.33, bottom) in their low (20 °C) and high (*ca.* 50 °C) temperature structural phases.

σ* orbitals into the excited electronic state.[53] With increased branching, the relative intensities of the Si−C and Si−Si stretch vibrations decrease, while their bandwidths increase. The largest change occurs in going from **3** to **4**. These results show that incorporation of branching points not only reduces side chain crystallinity, but also main chain regularity. It is furthermore noteworthy that the shapes and intensities of the Si−Si and Si−C stretch modes are related to the extent of σ-conjugation along the silicon backbone.[53] Consequently, it is concluded that insertion of branching sites diminishes the degree of σ-conjugation, which is consistent with UV, fluorescence, and conductivity data reported below.

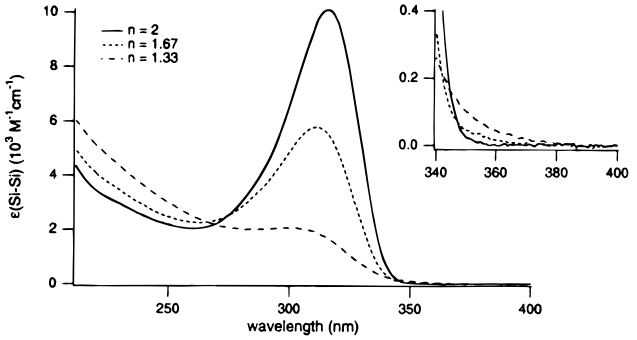

Figure 5. UV spectra of polymers **1** (n = 2), **3** (n = 1.67), and **4** (n = 1.33) in room temperature THF solution. The inset shows an enlargement of the network absorption tail.

Table 3. Electronic Absorption Properties of Polymers $[Si(C_6H_{13})_n]_m$

polymer (n)	λ_{max}[a] (nm)	ϵ(Si-Si)[a] (M^{-1} cm^{-1})	λ_{sol}^{LT}[b] (nm)	λ_{sol}^{HT}[c] (nm)	λ_{ss}^{LT}[d] (nm)	λ_{ss}^{HT}[e] (nm)
1 (2)	315	10 200	353	318	377	318
2 (1.95)	315	10 100	355	318	373	316
3 (1.67)	312	5 770	352	317	369	309
4 (1.33)	301	2 050	350	315	357	303

[a] In room temperature THF solution. [b] λ_{max} in hexane solution at −50 °C. [c] λ_{max} in hexane solution at 0 °C. [d] λ_{max} in the solid state (film) at 24 °C. [e] λ_{max} in the solid state (film) at 45 °C.

Above the phase transition temperature the sharp peaks have been transformed into broad bands. Although this effect is less dramatic for polymers with a high degree of branching, the backbone order in all polymers is reduced after the transition. In accordance with the IR results, the peak heights of side chain Raman bands (1500−700 cm^{-1} region) decrease as well during the thermal transition. It is notable that incorporation of 67% branching sites (**4**, n = 1.33) exerts a similar influence on the vibrational spectra of **1** as the solid−mesophase transition.

To summarize, the WAXD, DSC, IR, and Raman data all show that incorporation of branching points gradually reduces the degree of crystallinity of linear **1**. In all polymers a thermal transition occurs, which becomes however less pronounced with increased branching.

Optical Properties in Solution. UV spectra of polymers **1**−**4** in room temperature THF solution exhibit the typical sharp σ−σ* absorption around 315 nm of linear polysilylenes (Figure 5). With increased branching, a small hypsochromic shift is found, while the intensity decreases strongly (Table 3). Simultaneously, the contribution from a broad featureless band extending into the visible region, originating from the branched silicon moieties,[9,10,13,14] increases. This contribution is for the greater part responsible for the observed hypsochromic shifts of the σ−σ* bands but is still rather small in polymer **4** when compared to the spectrum of poly(n-hexylsilyne).[9,10,13,14]

It should be stipulated that the broad absorption tail is absent in the UV spectra of oligomeric dendritic silanes which contain more silyne than silylene subunits.[34] In this regard, the absorption spectra of oligomeric and polymeric hybrid polysilylene−polysilyne networks are in reasonable mutual agreement. However, the large extinction coefficients found in the dendritic silanes, attributed to a redundancy of conjugation paths,[32] are not found for branched polysilylenes **2**−**4**; their σ−σ* extinction coefficients are smaller than

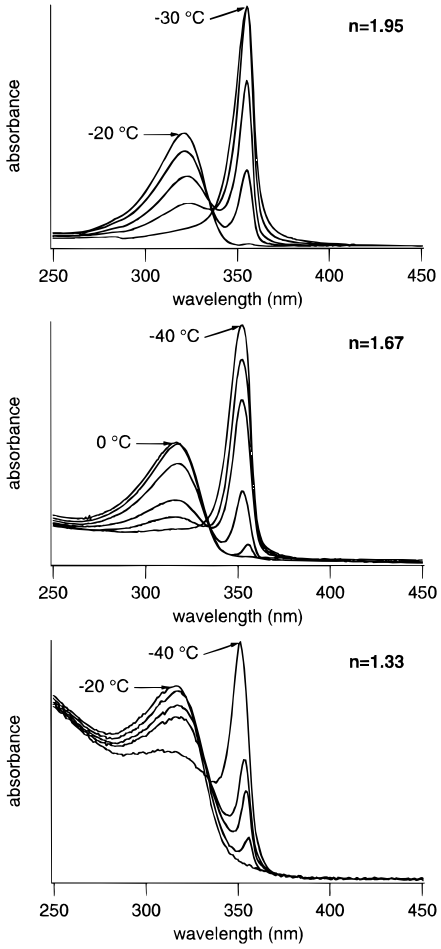

Figure 6. Solution thermochromism in hexane of polymers **2** ($n = 1.95$, top), **3** ($n = 1.67$, middle), and **4** ($n = 1.33$, bottom). Spectra were successively recorded at −20, −22, −24, −26, and −30 °C for **2**, at −40, −29, −20, −10, and 0 °C (thus upon heating) for **3**, and at −20, −25, −30, −35, and −40 °C for **4**.

in linear **1**. Thus, whereas the $\sigma-\sigma^*$ absorption maximum of **4** is denotative of polymeric UV behavior, the ϵ value of 2050 per Si−Si bond is lower than that of permethylated short oligosilylenes.[54,55] Furthermore, the UV properties of branched poly(*n*-hexylsilylene)s differ markedly from those of poly(*n*-hexylmethylsilylene) with *n*-hexylsilyne branching points,[13] where the linear $\sigma-\sigma^*$ band already disappears with 25% branching. Furthermore, in poly(methylphenylsilylene-*co*-phenylsilyne)s the linear $\sigma-\sigma^*$ absorption characteristics are hardly present in polymers incorporating 60% or more phenylsilyne branching points.[12]

In solution polymers **1**−**4** display thermochromic transitions; *i.e.*, their electronic absorption spectra change with temperature. In hexane reversible transitions occur between −20 and −30 °C for polymers **1** and **2**, but for polymers **3** and **4** the transition temperature range is broader (−10 to −40 °C, Figure 6). In these temperature ranges, maxima of the $\sigma-\sigma^*$ bands shift abruptly from 315−318 to 350−354 nm (Table 3), while extinction coefficients increase and bands narrow. The thermochromic shift is thus of comparable magnitude for all polymers. The presence of an isosbestic point during the transition of polymers **1**−**4** suggests a discrete transformation between the two phases without involvement of an intermediate phase.

The known solution thermochromism of **1** has been attributed to formation of *all-trans* segments (coil to rod transition) at lower temperatures (*vide infra*), presumably *via* a unimolecular conformational change.[56,57] Of all possible conformations, the *all-trans* segments possess the narrowest band gap and highest extinction coefficients. Apparently, a similar transition also occurs in the branched polymers. However, the residual absorption at the high temperature (HT) maximum in the LT phase increases with branching. This indicates that whereas in polymers **1** and **2** the transition is an all-chain event, in the branched polymers **3** and **4** a transition of only a part of the polymer is observed. This behavior can be understood by assuming that the partially branched polymers consist of conformationally rigid ring (network-type) structures which are interconnected by flexible linear fragments.[12,13,58]

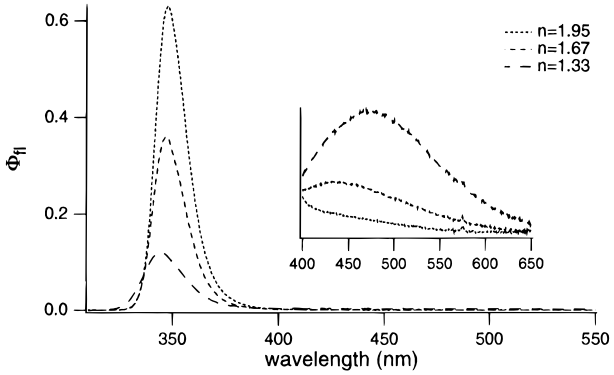

Figure 7. Room temperature fluorescence spectra (solvent THF) of polymers **2**−**4** upon 300 nm excitation. Maxima are scaled to the fluorescence quantum yield. The inset displays an enlargement of the weak emission originating from the branching sites after 350 nm excitation.

Fluorescence spectra of polymers **1**−**4** in room temperature THF solution are dominated by the narrow linear $\sigma-\sigma^*$ emission around 345 nm (Figure 7, Table 4). The excitation wavelength dependence of this emission is small.[59] The lifetime of the (σ,σ^*) emissive state is 300 ps, in line with other reported data,[13] and appears to be independent of the degree of branching. In the hybrid polymers **3** and **4** an additional broad emission around 440 nm is visible, which gains intensity and shifts to lower energies with a higher degree of branching. A biexponential fluorescence decay is found. Similar observations were made previously for poly(methylphenylsilylene-*co*-phenylsilyne)s[12] and poly(*n*-hexylmethylsilylene) with *n*-hexylsilyne branching points.[13] The broad emission has been attributed to recombination of excitons trapped at branching sites and resembles the emission of amorphous semiconductors.[13,14] It is dependent on the excitation wavelength; upon longer wavelength excitation the relative intensity of the broad emission increases, while the peak maximum shifts bathochromic in the case of **4**. Hence, a variety of branching site chromophores, which can be populated independently, is present. Furthermore, the linear and branched parts of the polymers more or less behave as separate chromophores. This is corroborated by the different fluorescence lifetimes of the two emission types (Table 4) and the independence of the linear fluorescence lifetime from the degree of branching.

It is conspicuous that the $\sigma-\sigma^*$ emission is still dominant in polymer **4** ($n = 1.33$), whereas it was reported to be either absent or weak in poly(*n*-hexylmethylsilylene) with 5% hexylsilyne branching points incorporated (albeit at 20 K)[13] and poly(methylphenylsilylene) with 60% phenylsilyne subunits.[12] In branched polysilylenes, the broad emission originates from excitons generated in the linear moieties which subse-

Table 4. Fluorescence Properties and Conjugation Lengths of Polymers $[Si(C_6H_{13})_n]_m$ in Room Temperature THF Solution

polymer (n)	λ_{em}^{300} [a] (nm)	λ_{em}^{337} [a] (nm)	λ_{em}^{350} [a] (nm)	Φ_{fl} [b]	τ_{fl1} [c] (ns)	τ_{fl2} [d] (ns)	f [e]	τ_r (ns)	τ_{abs} (ns)	n_{conj}
1 (2)	340	344		0.65	0.3		0.127	0.46	7.8	17
2 (1.95)	347	344		0.63	0.3		0.123	0.48	8.1	17
3 (1.67)	346	344/*437*	434	0.36	0.3	0.3; 2	0.080	0.83	13.4	16
4 (1.33)	344	344/*440*	470	0.12	0.3	0.7; 7	0.043	2.50	21.0	8

[a] Emission maxima upon excitation at 300, 337, and 350 nm, respectively. Values in italics denote maxima of the broad emission. [b] Fluorescence quantum yield of the linear $\sigma-\sigma^*$ emission. [c] Fluorescence lifetime of the linear $\sigma-\sigma^*$ emission monitored at 360 nm. [d] Fluorescence lifetimes of the broad red shifted emission, monitored at 450 (**3**) and 430 (**4**) nm, respectively. [e] Oscillator strength obtained by numerical integration.

quently migrate to the branching sites at which they are trapped and undergo radiative relaxation.[13] Although the differences between the emissive properties of the various polysilylene−polysilyne copolymers have been previously attributed to differences in molecular weight and the extension of the silicon network structure,[12] we believe that the nature of the side chains plays a decisive role. Apparently, in our polymers the hexylsilyne units do not severely affect the dihexylsilylene conjugation path, whereas in poly(hexylmethylsilylene) and poly(methylphenylsilylene) the respective hexylsilyne and phenylsilyne branching points act as efficient exciton traps. This is supported by the UV spectra of the various hybrid networks. That branching points can be a part of the conjugation part is indicated by the fluorescence spectrum of the oligosilylene dendrimer $[2,2\text{-}(Me_3Si)_2Si_3Me_5]_3SiMe$, which exhibits both a linear and a network silicon backbone emission band.[34] However, the relative intensity of the network emission band in the dendritic oligosilylene is higher.

The conjugation length, *i.e.*, the number of silicon atoms over which an exciton is delocalized, can be assessed from the fluorescence quantum yield, fluorescence lifetime, and the oscillator strength of the $\sigma-\sigma^*$ transition.[59,60] The oscillator strength f can be obtained from the integrated absorption intensity by:

$$f = (4.315 \times 10^{-9}) \int \epsilon(\text{Si}-\text{Si})\, d\nu \qquad (1)$$

and the radiative lifetime based on the absorption by one Si−Si bond (τ_{abs}) is given by

$$\tau_{abs} = \frac{1}{\nu_{max}^2 f} \qquad (2)$$

in which ν_{max} represents the wavenumber at maximum absorption. The radiative lifetime of excitons delocalized over the silicon backbone (τ_r) is related to the fluorescence quantum yield (Φ_{fl}) and lifetime (τ_{fl}):

$$\tau_r = \frac{\tau_{fl}}{\Phi_{fl}} \qquad (3)$$

Finally, the conjugation length n_{conj} is given by

$$n_{conj} = \frac{\tau_{abs}}{\tau_r} \qquad (4)$$

Results are collected in Table 4.[61] It is seen that fluorescence quantum yields of the $\sigma-\sigma^*$ emission decrease strongly with increased branching, while fluorescence lifetimes are essentially constant. Hence, radiationless decay becomes more dominant with increased branching. Whereas it is expected that excitations are strongly localized in totally branched **5**,[14,62] they appear to be delocalized over a considerable number of silicon atoms in the partially branched polymers. The conjugation length for **3** is only slightly shorter than those for **1** and **2**. Since the probability that in **3** ($n = 1.67$) and **4** ($n = 1.33$) di-*n*-hexylsilylene blocks of lengths comparable to the conjugation lengths exist is very low, the conjugation path has to contain *n*-hexylsilyne subunits. It follows that the (σ,σ^*) excited state is only moderately deactivated by trapping of excitons at branching points. The partially branched polymers thus possess the band gap of silicon network systems, at the expense of only a limited decrease in conjugation length. Unfortunately, the narrow band gaps and long conjugation lengths are related to uncoupled photophysical phenomena, which renders the delocalized σ-system inaccessible to excitons generated at branching sites.

Solid State Optical Properties. The thermal transitions of polymers **1**−**4** as revealed by DSC and both IR and Raman spectroscopy are accompanied by solid state thermochromism. Thin film UV spectra of these polymers show an abrupt change in the position of the sharp "linear" band in the temperature range of the transition observed with DSC (Figure 8, Table 3). In the LT phase, the $\sigma-\sigma^*$ maximum of polymer **1** is situated at 377 nm (literature: 370−375 nm[18]) and a shoulder around 355 nm can be distinguished. As the degree of branching increases, the shoulder at 355 nm becomes more pronounced, and in polymer **4** ($n = 1.33$) the maximum is situated at 357 nm while no distinct absorption around 375 nm is discernible anymore. This implies that in the branched polymers a backbone conformation other than the *all-trans* is preferred; the maximum observed for **4** is reminiscent of a *TGTG′* backbone conformation.[18] Another possibility is that a decrease of the length of *all-trans* segments is responsible for the hypsochromic shift. However, in this case the appearance of discrete shoulders would not be expected.

In the LT spectra of polymers **3** and **4** bands situated at the HT maxima are still present, as was observed in solution as well. In agreement with the DSC and vibrational studies, only a fraction of the branched silicon backbones undergoes the thermally induced conformational change, which is also in line with their increased amorphous character (*vide supra*). The suggestion of the presence of isosbestic points in the temperature dependent UV spectra in Figure 8 again implies a discrete transformation between two phases.

As is well documented, the absorption maximum of **1** ($n = 2$) shifts from 375−370 to 318−317 nm upon heating from the crystalline to the liquid crystalline phase.[46,63] Introduction of branching points leads to a hypsochromic shift of the maxima in the HT phase. This shift is assigned to an increased contribution of the network absorption rather than to conformational phenomena. Note that the maxima of the HT solid state spectra are more strongly influenced by the network

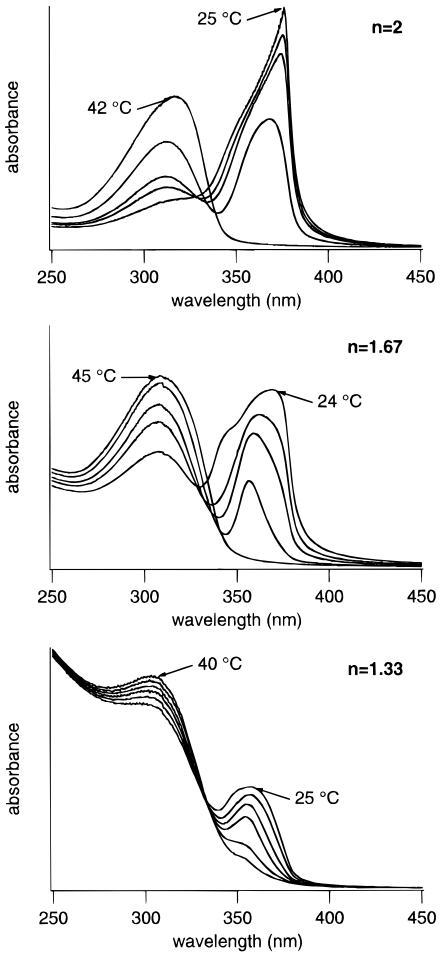

Figure 8. Solid state thermochromism of polymers **1** ($n = 2$, top), **3** ($n = 1.67$, middle), and **4** ($n = 1.33$, bottom). Spectra were successively recorded at 25, 30, 35, 40, and 42 °C for **1**, at 24, 32, 35, 38, and 45 °C for **3**, and at 25, 28, 31, 37, and 40 °C for **4**.

absorption tail than the maxima of the relatively well-defined, sharp HT solution spectra. Nevertheless, the HT solid state maxima bear a striking resemblance to the maxima in THF solution.

The maximum of **4** (357 nm) and the shoulder at 345−355 nm of the other polymers in the LT *solid state* spectra are found in the same region as the LT *solution* maxima of **1**−**4** (350−355 nm). Consequently, the backbone structures of polymers **1**−**4** in LT solutions correspond to a discrete solid state conformation, which is not *all-trans* (λ_{max} 375 nm) but presumably *TGTG′*. The assignment of the solution thermochromism of polymer **1** to formation of *all-trans* segments (coil to rod transition) at low temperatures[57] is therefore unlikely to be correct.

The thermal transitions have a remarkable effect on the solid state (film) fluorescence as well. As shown in Figure 9, emission maxima of **1**−**4** (polymer **2** behaves similarly to **1**) all shift from 380−382 nm in the LT phase to 345−348 nm in the HT phase. The LT spectra show weak additional bands in the region of the HT maxima. The LT maxima are in line with reported data on the solid phases of poly(di-*n*-hexylsilylene) (**1**)[64,65] and are characteristic of emission from *all-trans* segments. It is conspicuous that in the LT phases emission maxima are identical, whereas the LT solid state UV spectra show distinct differences. Regardless the LT chain conformation, the mobility of excitons in the silicon backbones appears to enable population of the lowest

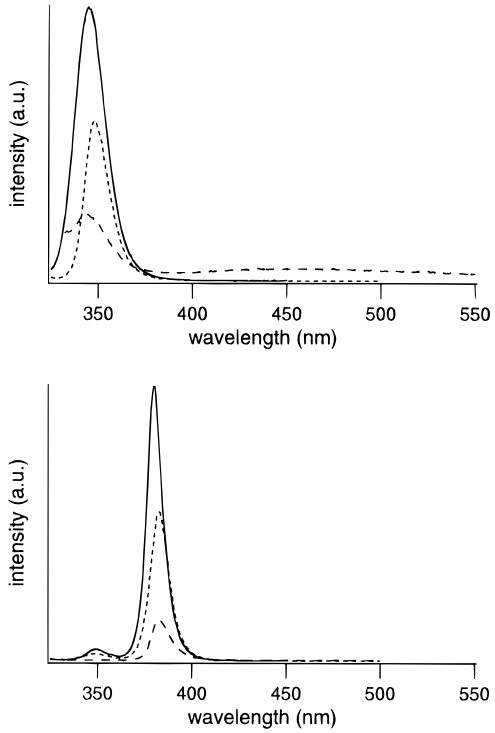

Figure 9. Solid state (film) fluorescence spectra of polymers **1** ($n = 2$, —), **3** ($n = 1.67$, - - -), and **4** ($n = 1.33$, — —) in their high (top) and low temperature (bottom) phases. Ordinates are arbitrarily scaled. High temperature maxima are 345 (**1**), 348 (**3**), and 345 (**4**) nm, and low temperature maxima are 380 (**1**), 382 (**3**), and 382 (**4**) nm. Excitation wavelength 320 nm.

lying excited chromophores, *i.e.*, segments of *all-trans* conformation emitting around 382 nm in each polymer. Although the LT solid state UV spectrum of **4** exhibits its maximum at 357 nm, some absorption is present around 375 nm, indicative of the presence of *all-trans* segments. With regard to the fact that prominent *all-trans* emission is observed for the structurally disordered hybrid networks, energy transfer must be very efficient. As solid state phenomena are dealt with, interchain energy transfer is not unlikely to contribute significantly.

The HT fluorescence maxima of **1**−**4** correspond to the values in solution. In **4** the linear emission is weak and the broad emission around 450 nm assigned to the branching sites is clearly visible; the latter emission is still very weak in **3**. Since no emission around 382 nm fluorescence is discernible, excited segments with an *all-trans* geometry are not populated in the HT forms.

Charge Migration. In order to investigate charge carrier mobilities in the hybrid networks, we used the pulse-radiolysis time-resolved microwave conductivity (PR-TRMC) technique.[38−40] This is a contactless high frequency conductivity technique, which implies that grain boundary and space charge effects can be eliminated. Samples are ionized using pulsed irradiation with 3-MeV electrons from a Van de Graaff accelerator. Upon ionization, which occurs predominantly in the hexyl side chains, electron-hole pairs (e^--h^+) undergo diffusional separation and are scavenged by the silicon backbone. The conductivity change is then monitored by time-resolved measurement of the change in microwave power reflected by the sample. The measured micowave conductivity reflects the charge carrier motion within the structural domains of a sample and is strongly related to the presence of structural order. In polysilylenes TRMC monitors predominantly charge

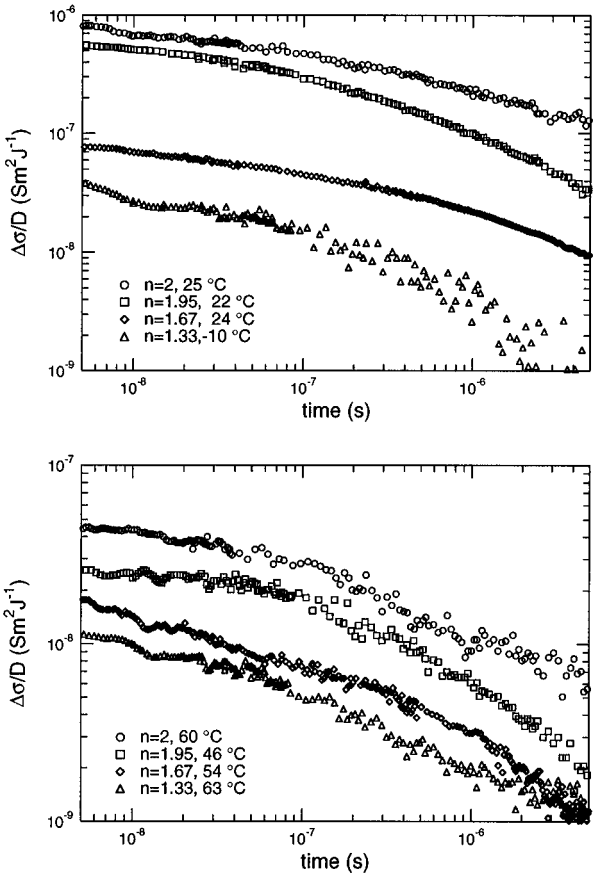

Figure 10. Dose normalized conductivity ($\Delta\sigma/D$) transients of polymers **1**-**4** after irradiation with 0.5−10 ns pulses of 3-MeV electrons. The top panel displays transients obtained in the low temperature phase, the bottom one those obtained in the high temperature phase. Note that the ordinates of the two panels are not equal.

Table 5. Conductive Properties of Polymers $[Si(C_6H_{13})_n]_m$

polymer (n)	phase	T (°C)	$\Delta\sigma_{eop}/D$ (10^{-8} S m^2 J^{-1})	$\sum\mu_{min}$ (10^{-7} m^2 V^{-1} s^{-1})	$t_{1/2}$ (ns)	$\langle x\rangle$ (10^{-8} m)
1 (2)	LT	24	71	150	450	28
1 (2)	HT	60	3.8	8.0	150	6.8
2 (1.95)	LT	24	53	110	150	24
2 (1.95)	HT	60	3.3	7.0	300	6.3
3 (1.67)	LT	24	7.6	16	150	9.0
3 (1.67)	HT	60	1.7	3.6	100	4.5
4 (1.33)	LT	−25	3.6	7.6	100	5.7
4 (1.33)	HT	60	1.0	2.1	100	3.5

migration along the silicon backbones;[28] chain to chain hopping plays only a minor role. With the PR-TRMC technique it is not possible to discriminate between electron and hole conduction; it is however known that holes are the predominant charge carriers in polysilylenes.[20,24]

Radiation induced TRMC transients of polymers **1**−**4** in the LT and HT temperature phases are shown in Figure 10. The transients are normalized to the volume dose D (J·m^{-3}) deposited in the sample by the irradiation pulse. It is seen in Figure 10 that irrespective of the degree of branching charge carriers are long-lived, up to microseconds and longer. Similar disperse (*i.e.*, multiexponential) decay kinetics, as designated by the roughly comparable first half lifetimes $t_{1/2}$, are observed for all polymers (Table 5). Remarkably, the charge carriers are thus much longer lived than expected when the branching points act as efficient charge carrier traps. In the latter case $t_{1/2}$ would be greatly affected by the introduction of branching sites. From the similarity in the transient decay kinetics we attribute differences in conductivity to changes in charge carrier mobilities rather than to the occurrence of strong trapping of charge carriers at branching points.

Figure 10 demonstrates that the magnitude of the dose normalized conductivity signals is lowered by incorporation of branching points. In addition, upon going from the LT to the HT phase, a decrease in conductivity occurs. The temperature dependence of the dose normalized conductivity at the end of the pulse, $\Delta\sigma_{eop}/D$, is shown in more detail in Figure 11. The thermal transitions of polymers **1**−**4** are associated with an abrupt decrease of $\Delta\sigma_{eop}/D$ as has been observed earlier for a series of poly(di-*n*-alkylsilylenes).[42] The transition temperatures and hystereses coincide fairly with those found from the DSC measurements. The decrease of $\Delta\sigma_{eop}/D$ at the transition of **1** and **2** is more than an order of magnitude. For **3** and **4** a much smaller effect is observed, being in accordance with the decrease of transition enthalpy and the less pronounced solid state UV thermochromism upon introduction of branching sites. As in both temperature phases $t_{1/2}$ values are of comparable magnitude, the conductivity decay is merely unaffected by the thermal transitions.

It is illustrative to consider charge carrier mobilities μ. The sum of the positive and negative charge carrier mobilities ($\sum\mu$) is directly related to the conductivity change at the end of the irradiation pulse $\Delta\sigma_{eop}$ according to

$$\Delta\sigma_{eop} = eN_p\sum\mu \tag{5}$$

where e represents the elementary charge and N_p is number density of charge carriers, electron-hole pairs (e^--h^+), formed upon irradiation. Since it is likely that a part of the initially formed (e^--h^+) pairs recombines on a subnanosecond time scale, a lower limit to $\sum\mu$, $\sum\mu_{min}$, is obtained which can be calculated from $\Delta\sigma_{eop}/D$ *via*[27]

$$\sum\mu_{min} = E_p\frac{\Delta\sigma_{eop}}{D} \tag{6}$$

where E_p is the energy absorbed per (e^--h^+) pair formed ($E_p = D/eN_p$). For poly(di-*n*-hexylsilylene) (**1**), E_p has been estimated to be 21 eV,[27] a value that is adopted for polymers **2**−**4** as well.[66] Mobilities obtained upon use of this value are collected in Table 5.

A high value of $\sum\mu_{min}$ of 1.5×10^{-5} m^2 V^{-1} s^{-1} is found for the crystalline phase of **1**.[27,29] This value is close to that of 1×10^{-4} m^2 V^{-1} s^{-1} found for amorphous silicon. In the presence of branching sites $\sum\mu_{min}$ is lowered. Already with 5% branching a significant decrease of $\sum\mu_{min}$ is observed. This finding corresponds nicely to the presence of amorphous regions in this polymer as revealed by WAXD. The value obtained for **4**, 7.6×10^{-7} m^2 V^{-1} s^{-1}, is more than an order of magnitude lower than that for the linear polymer **1**. Thus, whereas incorporation of branching points shifts the band gap toward that of amorphous silicon, charge carrier mobilities move into the opposite direction. Nonetheless, the mobility of charge carriers in **4** is still considerable.

During the thermal transition of **1** $\sum\mu_{min}$ decreases more than an order of magnitude. This compares reasonably with a theoretical study on polysilylenes, which revealed an increase in the effective charge carrier mass with a factor of 60 when going from an *all-trans* to an *all-gauche* backbone.[42,67] As expected

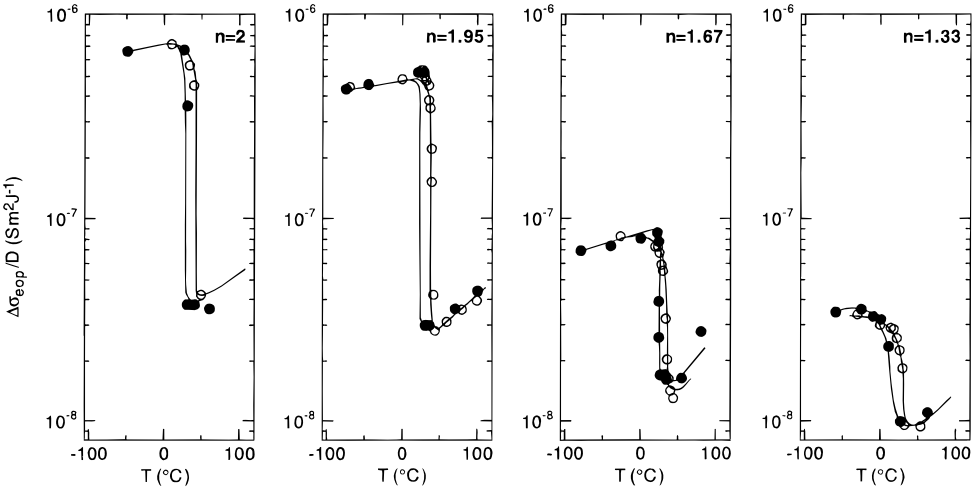

Figure 11. Temperature dependence of the charge carrier mobilities of polymers **1**−**4**. Open circles correspond to values obtained on heating, filled circles to values obtained on cooling.

from the $\Delta\sigma_{eop}/D$ data, the effect of the phase transition on the mobility is still considerable for **2**, while it is much smaller for the strongly branched polymers **3** and **4**. It is not surprising that mobilities in the already strongly disordered HT phases are less affected by incorporation of branching points than is the case in the relatively well ordered LT phases.

Thus, in both temperature phases the presence of *n*-hexylsilyne subunits decreases $\sum\mu_{min}$. It has to be emphasized that this is not a consequence of efficient charge carrier trapping, as evidenced by the comparable decay kinetics observed for all polymers in both temperature phases. The point is further supported by an estimate of the average displacement $\langle x\rangle$ of charge carriers, which can be assessed on assuming one-dimensional charge carrier diffusion *via*

$$\langle x\rangle^2 = \frac{2\mu k_B T}{e} t \qquad (7)$$

In this expression k_B is the Boltzmann constant, T the temperature (in K), and t the time. Results obtained after taking $t = 100$ ns (close to the first half lifetimes of the conductivity transients) and $\sum\mu_{min}$ for μ are given in Table 5. As is evident from eq 7, the travel distances qualitatively follow the trends in mobilities: they decrease both with increased branching and upon going from the LT to the HT phases. It is however seen that even in the most unfavorable case, *i.e.*, the HT phase of polymer **4**, charge carriers migrate over some 150 Si−Si bonds (using a Si−Si bond length of 2.35 Å).[32,34] This implies that approximately 100 branching sites are passed over in the relative short period of 100 ns after the excitation pulse. Moreover, it must be kept in mind that actual traveled distances are larger than the average displacement $\langle x\rangle$, and that thus a larger number of branching sites must be passed.

The PR-TRMC results unequivocally show that the branching points are part of the conjugation path, in agreement with conclusions derived from the UV and fluorescence measurements. However, their presence systematically lowers the charge carrier mobilities, which is attributed to a cooperation of two factors. First, the presence of branching points lowers the mobility in the LT phase by inducing a distortion of the *all-trans* polymer backbone. It has been recognized earlier that conformational defects such as *gauche* kinks offer resistance to the motion of holes along the silicon backbone.[18] The associated decrease of $\sum\mu_{min}$ corresponds qualitatively to the decrease of the conjugation length in solution and the hypsochromic UV shifts (in a series of polysilylenes a linear correlation is found between $\sum\mu_{min}$ and solution UV maxima).[42] The reduction of $\sum\mu_{min}$ is however more pronounced than anticipated from the decrease in conjugation length and the magnitude of the UV shift.[42] This is for instance illustrated by the fact that incorporation of 67% branching sites ($n = 1.33$) has an equal strong effect on the mobility as the solid−mesophase transition of **1**, whereas the solid state UV shift is significantly smaller in the former case. Thus, apart from influencing the backbone structure, branching points are supposed to behave as scattering points for charge carriers; shallow trapping and detrapping at branching points may occur. This scattering effect is in particular observable in the HT forms of the polymers. Although the mesophase of **1** is already disordered, branching still reduces the charge carrier mobilities.

Finally, the PR-TRMC results also provide evidence that branching points are uniformly distributed in the branched polysilylene structures. Owing to the large sensitivity of PR-TRMC responses to ordered structures, $\Delta\sigma_{eop}$ and mobility values of the branched polymers would have been much closer to the values obtained for polymer **1** if large amounts of long linear segments are present in the branched structures.

Conclusions

The incorporation of *n*-hexylsilyne branching points into poly(di-*n*-hexylsilylene) induces a loss of crystallinity, but partial crystallinity remains present. Simultaneously, the prominence of the first-order phase transition decreases. Branched *n*-hexyl substituted polysilylenes furthermore combine the photophysical properties of linear polysilylenes and *pseudo*-2-dimensional polysilynes, although the polysilyne characteristics are not proportional to the relative number of branching points. Polymers **1**−**4** behave thus more or less as *quasi*-linear silicon-based polymers, which is manifested by the appearance of $\sigma-\sigma^*$ absorption, $\sigma-\sigma^*$ emission, and solution and solid state thermochromism, respectively. In addition, in polymers **3** and **4** the narrow band gap of 2-D silicon systems is accompanied by a perseverance of the favorable linear exciton delocalization. Charge carrier mobilities in the strongly branched polysilylenes are still considerable, although

they are reduced with a factor of 10−20 in comparison to the linear polymer; the branching points act as scattering points for charge carriers.

In terms of σ-conjugation, it is apparent from the smaller band gaps that incorporation of the 2-dimensional branching points increases the σ-conjugation in the ground state. On the other hand, it can be stated that the extent of σ-conjugation of the *quasi-linear* segments is reduced. This is however more related to excited state phenomena; the presence of branching sites diminishes the number of silicon atoms over which excitons are delocalized. This is qualitatively in line with the role of the branching sites as scattering points for charge carriers.

The combination of high charge carrier mobilities and mainly amorphous character in branched polysilylenes **3** and **4** renders them attractive materials for application as photoreceptors in xerography.[25]

Acknowledgment. The authors thank J. van Slageren, M. Versluis, and E. S van de Windt (Utrecht University) for synthetic contributions and help with WAXD and Raman spectroscopy, respectively. Dr. J. M. Warman and G. H. Gelinck (IRI, Delft University of Technology) are gratefully acknowledged for stimulating discussions and determinination of fluorescence lifetimes.

References and Notes

(1) Matsumoto, N.; Takeda, K.; Teramae, H.; Fujino, M. In *Silicon-Based Polymer Science*; Zeigler, J. M., Fearon, F. W. G., Eds.; Advances in Chemistry Series 224; American Chemical Society: Washington, DC, 1990; p 515.
(2) Brus, L. *J. Phys. Chem.* **1994**, *98*, 3575.
(3) Canham, L. T. *Appl. Phys. Lett.* **1990**, *57*, 1046.
(4) Meulenkamp, E. A.; Cleij, T. J.; Kelly, J. J. *J. Electrochem. Soc.* **1994**, *141*, 1157.
(5) Prokes, S. M.; Glembocki, O. J. *Mater. Chem. Phys.* **1993**, *35*, 1.
(6) Sailor, M. J.; Kavanagh, K. L. *Adv. Mater.* **1992**, *4*, 432.
(7) Barzoukas, M.; Fort, A.; Klein, G.; Serbutoviez, C.; Oswald, L.; Nicoud, J. F. *Chem. Phys.* **1992**, *164*, 395.
(8) Kanemitsu, Y. *J. Non-Cryst. Solids* **1993**, *164−166*, 1279.
(9) Bianconi, P. A.; Weidman, T. W. *J. Am. Chem. Soc.* **1988**, *110*, 2342.
(10) Bianconi, P. A.; Schilling, F. C.; Weidman, T. W. *Macromolecules* **1989**, *22*, 1697.
(11) Furukawa, K.; Fujino, M.; Matsumoto, N. *Macromolecules* **1990**, *22*, 3423.
(12) Watanabe, A.; Miike, H.; Tsusumi, Y.; Matsuda, M. *Macromolecules* **1993**, *26*, 2111.
(13) Wilson, W. L.; Weidman, T. W. *J. Phys. Chem.* **1991**, *95*, 4568.
(14) Wilson, W. L.; Weidman, T. W. *Synth. Met.* **1992**, *49−50*, 407.
(15) Sasaki, M.; Matyjaszewski, K. *J. Polym. Sci., Part A: Polym. Chem.* **1995**, *33*, 771.
(16) Amorphous silicon structures can be formed from polysilynes upon heat treatment: Watanabe, A.; Nagai, Y.; Matsuda, M.; Suezawa, M.; Sumino, K. *Chem. Phys. Lett.* **1993**, *207*, 132.
(17) Maxka, J.; Chrusciel, J.; Sasaki, M.; Matyjaszewski, K. *Macromol. Symp.* **1994**, *77*, 79.
(18) Miller, R. D.; Michl, J. *Chem. Rev.* **1989**, *89*, 1359.
(19) *Silicon-Based Polymer Science*; Zeigler, J. M., Fearon, F. W. G., Eds.; Advances in Chemistry Series 224; American Chemical Society: Washington, DC, 1990.
(20) Fujino, M. *Chem. Phys. Lett.* **1987**, *136*, 451.
(21) West, R.; David, L. D.; Djurovich, P. I.; Stearly, K. I.; Srinivasan, K. S. V.; Yu, H. *J. Am. Chem. Soc.* **1981**, *103*, 7352.
(22) Kajzar, F.; Messier, J.; Rosilio, C. *J. Appl. Phys.* **1986**, *60*, 3040.
(23) Baumert, J. C.; Bjorklund, G. C.; Jundt, D. H.; Jurich, M. C.; Looser, H.; Miller, R. D.; Rabolt, J.; Sooriyakumaran, R.; Swalen, J. D.; Twieg, R. J. *Appl. Phys. Lett.* **1988**, *54*, 1147.
(24) Kepler, R. G.; Zeigler, J. M.; Harris, L. A.; Kurtz, S. R. *Phys. Rev. B* **1987**, *35*, 2818.
(25) Abkowitz, M. A.; Stolka, M.; Weagly, R. J.; McGrane, K. M.; Knier, F. E. In *Silicon-Based Polymer Science*; Zeigler, J. M., Fearon, F. W. G., Eds.; Advances in Chemistry Series 224; American Chemical Society: Washington, DC, 1990; p 467.
(26) Yokoyama, K.; Notsu, S.; Yokoyama, M. *J. Chem. Soc., Chem. Commun.* **1990**, 805.
(27) Frey, H.; Möller, M.; de Haas, M. P.; Zenden, N. J. P.; Schouten, P. G.; van der Laan, G. P.; Warman, J. M. *Macromolecules* **1993**, *26*, 89.
(28) van der Laan, G. P.; de Haas, M. P.; Hummel, A.; Frey, H.; Sheiko, S.; Möller, M. *Macromolecules* **1994**, *27*, 1897.
(29) van der Laan, G. P.; de Haas, M. P.; Warman, J. M.; Frey, H.; Möller, M. *Mol. Cryst. Liq. Cryst.* **1993**, *236*, 165.
(30) van der Laan, G. P.; de Haas, M. P.; van Walree, C. A.; van Slageren, J.; Jenneskens, L. W.; Frey, H. *Macromol. Symp.* **1996**, *102*, 355.
(31) Abkowitz, M. A.; McGrane, K. M.; Knier, F. E.; Stolka, M. *Mol. Cryst. Liq. Cryst.* **1990**, *183*, 157.
(32) Lambert, J. B.; Pflug, J. L.; Stern, C. L. *Angew. Chem., Int. Ed. Engl.* **1995**, *34*, 98.
(33) Sekiguchi, A.; Nanjo, M.; Kabuto, C.; Sakurai, H. *J. Am. Chem. Soc.* **1995**, *117*, 4195.
(34) Suzuki, H.; Kimata, Y.; Satoh, S.; Kuriyama, A. *Chem. Lett.* **1995**, 293.
(35) Blaauw, M. *Nucl. Instrum. Methods Phys. Res.* **1994**, *A353*, 269.
(36) de Bruin, M.; Kortenhoven, P. J. M. *Anal. Chem.* **1972**, *44*, 2382.
(37) Eaton, D. F. *Pure Appl. Chem.* **1988**, *60*, 1107.
(38) Warman, J. M.; de Haas, M. P.; Wentinck, H. M. *Radiat. Phys. Chem.* **1989**, *34*, 581.
(39) Warman, J. M.; de Haas, M. P. In *Pulse Radiolysis*; Tabata, Y., Ed.; CRC: Boca Raton, 1991; p 101.
(40) Schouten, P. G. Ph.D. Thesis, Delft University of Technology, 1994.
(41) Schouten, P. G.; Warman, J. M.; de Haas, M. P. *J. Phys. Chem.* **1993**, *97*, 9863.
(42) van der Laan, G. P.; de Haas, M. P.; Hummel, A.; Möller, M.; Frey, H. *J. Phys. Chem.* **1996**, *100*, 5470.
(43) Matyjaszewski, K.; Greszta, D.; Hrkach, J. S.; Kim, H. K. *Macromolecules* **1995**, *28*, 59.
(44) Even the use of ultrasonified emulsions of sodium−potassium alloy as coupling agent followed by titration with *n*-hexylmagnesium bromide[10] and performing the entire workup procedure under argon did not result in oxygen free material. It should however be noted that due to technical limitations in contrast to the literature procedure the trichlorosilane monomer was added to the alloy instead of adding the alloy to the trichlorosilane monomer.[10] Although it should be kept in mind that determination of oxygen in silicon-based polymers by elemental analysis is subject to error since complete combustion is difficult (Kumar, K.; Litt, M. H. *J. Polym. Sci., Part C: Polym. Lett.* **1988**, *26*, 25; Kolbe, H., personal communication), the presence of oxygen in **5** was confirmed by neutron activation analysis, which gave an oxygen content of 20.0 ± 1.9%. The difficulty of determination of the oxygen content by elemental analysis is for instance indicated by the presence of Si−O bands in the 1000−1200 cm^{-1} region of the IR spectra of polymers **3** and **4**, where according to the elemental analyses no oxygen is present. We assign these Si−O bands to Si−O−CH_3 end groups, formed from unreacted Si−Cl groups during quenching with methanol and/or Si−O−Si bonds.[11,12] From ^{1}H NMR integral ratios of polymers **3**−**5** a methoxy group content of 5 mol % (**5**) and less than 2% (**3**, **4**) is estimated. Despite the presence of oxygen the photophysical properties of **5** are in accordance with data reported by others. The only discrepancy is the extinction coefficient for **5**; an ϵ value of 12 500 M^{-1} cm^{-1} at 300 nm has been reported[10] while we found ϵ = 2000 M^{-1} cm^{-1} at 300 nm. Therefore, the properties of **5** are not taken into consideration unless this is essential for the understanding of the behavior of the partially branched polysilylenes **2**−**4**.
(45) Jones, R. G.; Benfield, R. E.; Cragg, R. H.; Swain, A. C.; Webb, S. J. *Macromolecules* **1993**, *26*, 4878.
(46) Rabolt, J. F.; Hofer, D.; Miller, R. D.; Fickes, G. N. *Macromolecules* **1986**, *19*, 611.
(47) Unfortunately, the wax-like aggregation states of polymers **3** and **4** hampered their characterization by WAXD.
(48) KariKari, E. K.; Greso, A. J.; Farmer, B. L.; Miller, R. D.; Rabolt, J. F. *Macromolecules* **1993**, *26*, 3937.
(49) Weber, P.; Guillon, D.; Skoulios, A.; Miller, R. D. *J. Phys. (Paris)* **1989**, *50*, 793.
(50) Leites, L. A.; Bukalov, S. S.; Yadritzeva, T. S.; Mokhov, M. M.; Antipova, B. A.; Frunze, T. M.; Dement'ev, V. V. *Macromolecules* **1992**, *25*, 2991.

(51) The spectra reported by Rabolt *et al.*[46] do not exhibit the band splitting. Furthermore, relative band intensities are different, which we attribute to differences in experimental conditions.
(52) Hagemann, H.; Snyder, R. G.; Peacock, A. J.; Mandelkern, L. *Macromolecules* **1989**, *22*, 3600.
(53) Bukalov, S. S.; Leites, L. A.; Mozorov, V. A.; West, R.; Menescal, R. *Mendeleev Commun.* **1994**, 41.
(54) Gilman, H.; Atwell, W. H.; Schwebke, G. L. *J. Organomet. Chem.* **1964**, *2*, 369.
(55) Kumada, M.; Tamao, K. *Adv. Organomet. Chem.* **1968**, *6*, 19.
(56) Trefonas, P., III; Damewood, J., Jr.; West, R.; Miller, R. D. *Organometallics* **1985**, *4*, 1318.
(57) Harrah, L. A.; Zeigler, J. M. *J. Polym. Sci., Polym. Lett. Ed.* **1985**, *23*, 209.
(58) No clear-cut evidence favoring either a ring-like or dendritic structure of the branched polysilylenes was obtained. It was hoped that IR and Raman spectroscopy could reveal the presence of silicon ring structures, but signals of characteristic ring vibrations are too weak (Brough, L. F.; West, R. *J. Am. Chem. Soc.* **1981**, *103*, 3049) to allow a reliable identification. Tentatively, we prefer the ring-like network structure.
(59) Michl, J.; Downing, J. W.; Karatsu, T.; Klingensmith, K. A.; Wallraff, G. M.; Miller, R. D. In *Inorganic and Organometallic Polymers*; Zeldin, M., Wynne, K., Allcock, H., Eds.; ACS Symposium Series 360; American Chemical Society: Washington, DC, 1988; Chapter 3.
(60) Kanemitsu, Y.; Suzuki, K.; Nakayoshi, Y.; Matsumoto, Y. *Phys. Rev. B* **1992**, *46*, 3916.
(61) One of the reviewers has pointed out that if the quantum yields Φ_{fl} decrease with the number of branching points, the fluorescence lifetimes τ_{fl} should alter as well. Although the time resolution of the lifetime measurement equipment (*ca.* 200 ps, see Schuddeboom, W., Ph.D. Thesis, Delft University of Technology, The Netherlands, 1994) is close to the fluorescence lifetimes of the branched polysilylenes, we are confident that lifetimes are equal for all polymers. Nevertheless, lifetime determinations using shorter time resolution could shed more light on this question; experiments are initiated. Another contemplation is that in the hybrid networks, of which the photophysical behavior is rather complex, the fluorescence lifetime τ_{fl} and quantum yield Φ_{fl} are possibly not strictly related *via* the common expressions (see text).
(62) For our sample of **5** we found $\Phi_{fl} = 0.005$, $\tau_{fl2} = 1$ and 10 ns (biexponential), $f = 0.038$, $\tau_r = 200$ ns, $\tau_{abs} = 25.1$ ns, and $n_{conj} = 0.1$.
(63) Miller, R. D.; Hofer, D.; Rabolt, J. F.; Fickes, G. N. *J. Am. Chem. Soc.* **1985**, *107*, 2172.
(64) Thorne, J. R. G.; Hochstrasser, R. M.; Zeigler, J. M. *J. Phys. Chem.* **1988**, *92*, 4275.
(65) Kyotani, H.; Shimomura, M.; Miyazaki, M.; Ueno, K. *Polymer* **1995**, *36*, 915.
(66) The E_p value of 21 eV for polymer **1** is based on the fact that ionization events occur mainly in its *n*-hexyl side chains;[27] as calculated from the relative number of electrons in the side chains and the polymer backbones, ionization events will occur for 88% in the *n*-hexyl side chains of polymer **1**. For **4** this percentage is 82%, implying that using $E_p = 21$ eV for all polymers is a reasonable approximation.
(67) Teramae, H.; Takeda, K. *J. Am. Chem. Soc.* **1989**, *111*, 1281.

MA960407H